Article

Developmental Cell

ROS burst prolongs transcriptional condensation to slow shoot apical meristem maturation and achieve heat-stress resilience in tomato

Graphical abstract

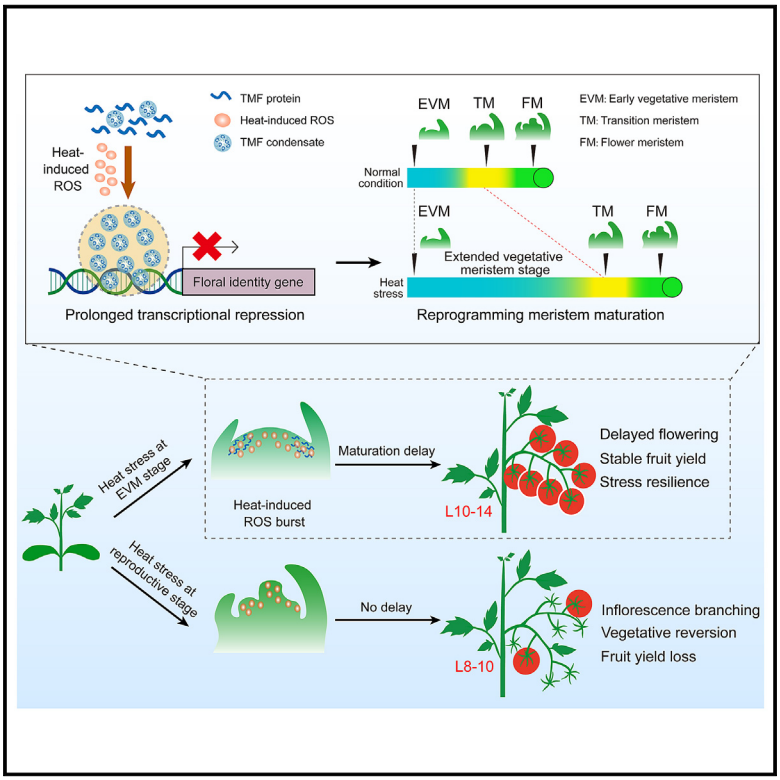

Highlights

- Tomato plants slow shoot meristem maturation to achieve heat-stress resilience
- Heat-induced ROS lengthen vegetative growth to avoid reproductive failure
- ROS burst prolongs transcriptional condensation of TMF to repress floral transition
- Transient phase-wise slow growth may be a bet-hedging strategy for heat resilience

Authors

Xiaozhen Huang, Nan Xiao, Yue Xie, Cao Xu

Correspondence

caoxu@genetics.ac.cn

In brief

Huang and Xiao et al. report that tomato plants slow shoot apical meristem maturation in response to heat stress to avoid reproductive failure. Heat-induced ROS prolong the transcriptional condensation of TMF, triggering transcriptional reprogramming that extends vegetative growth, which may represent a bet-hedging strategy for heat resilience in plants.

Huang et al., 2025, Developmental Cell *60*, 1–14
August 4, 2025
https://doi.org/10.1016/j.devcel.2025.03.007

CellPress

Developmental Cell

CellPress
OPEN ACCESS

Article

ROS burst prolongs transcriptional condensation to slow shoot apical meristem maturation and achieve heat-stress resilience in tomato

Xiaozhen Huang,[1,3,4] Nan Xiao,[1,2,3,4] Yue Xie,[1,2,3] and Cao Xu[1,2,3,5,*]

[1]Key Laboratory of Seed Innovation, Institute of Genetics and Developmental Biology, Chinese Academy of Sciences, Beijing 100101, China
[2]University of Chinese Academy of Sciences, Beijing 100049, China
[3]CAS-JIC Centre of Excellence for Plant and Microbial Science (CEPAMS), Institute of Genetics and Developmental Biology, Chinese Academy of Sciences, Beijing 100101, China
[4]These authors contributed equally
[5]Lead contact
*Correspondence: caoxu@genetics.ac.cn
https://doi.org/10.1016/j.devcel.2025.03.007

SUMMARY

The transition of the shoot apical meristem (SAM) from vegetative growth to flowering, a key step of angiosperm reproductive success, is highly vulnerable to heat stress. Overproduction of reactive oxygen species (ROS) is a hallmark of such environmental stresses, but how SAM exploits the extra ROS to achieve heat-stress resilience is largely unknown. Here, we report that tomato plants respond to heat-induced ROS burst by slowing down SAM maturation and lengthening the vegetative state to achieve heat resilience. Heat-induced extra ROS prolonged the transcriptional condensation status of TERMINATING FLOWER (TMF), a prion-like transcription repressor that undergoes phase separation by sensing hydrogen peroxide (H_2O_2), therefore temporarily delaying activation of flowering transition and extending vegetative growth. Loss-of-function of TMF, or base editing of a single cysteine residue that senses H_2O_2, abolishes heat resilience. Our findings demonstrate that transcriptional reprogramming triggered by ROS might be a molecular basis of plant developmental plasticity underlying heat-stress resilience.

INTRODUCTION

Rising temperature caused by global climate change poses a significant challenge to crop production, elevating interest in crop heat tolerance.[1] The response mechanism of heat stress (HS) on later stages of reproductive success, such as pollen development and fertilization, has been well documented in literatures.[2] However, the effects of HS on the shoot apical meristem (SAM) that harbors a group of stem cells located at the tip of each plant and generates all above-ground organs of higher plants, have been largely ignored.[3] Plants have evolved remarkable developmental plasticity to adapt to temperature changes and expand to diverse ecosystems, but our knowledge about the underlying molecular mechanisms of such plasticity is still very limited. Developmental plasticity is the organism's ability to adjust its growth and developmental processes in response to environmental cues in the time span of its lifetime, in contrast to passing beneficial genetic variations through natural selection across generations.[4,5] The plasticity of SAM development requires a mechanism to rewire the otherwise highly stable and precise SAM development program in response to environmental conditions.[3,6] Flowering transition, which marks the switch of SAM from vegetative to reproductive growth, is highly sensitive to HS.[7] Exposure to HS at this specific stage often leads to devastating consequences for reproductive development and seed/fruit setting as well as a substantial loss of crop yield.[8,9] However, at a molecular level, little is known about how exactly SAM canalizes environmental changes such as HS through adjustment of the maturation program to create the plasticity.

Plants have evolved sophisticated signaling pathways to respond to various environmental changes and achieve stress resilience. Accumulation of reactive oxygen species (ROS), such as hydrogen peroxide (H_2O_2) and superoxide ($O_2^{\cdot-}$), is a hallmark of responses to environmental stresses in plants.[10,11] On one hand, various proteins, such as heat-shock chaperones and signaling pathways, prevent ROS overproduction or remove non-functional proteins caused by oxidative damage to ensure developmental robustness under HS.[12–16] On the other hand, developmentally produced ROS can serve as beneficial signals for plant development and growth, including their significant roles in maintenance and differentiation of stem cells in the SAM and root apical meristem.[17–19] We recently found that developmentally produced H_2O_2 in the boundary domains of SAM induces the formation of disulfide bonds to trigger phase separation of a transcriptional repressor, TERMINATING FLOWER (TMF). The ROS-induced

Please cite this article in press as: Huang et al., ROS burst prolongs transcriptional condensation to slow shoot apical meristem maturation and achieve heat-stress resilience in tomato, Developmental Cell (2025), https://doi.org/10.1016/j.devcel.2025.03.007

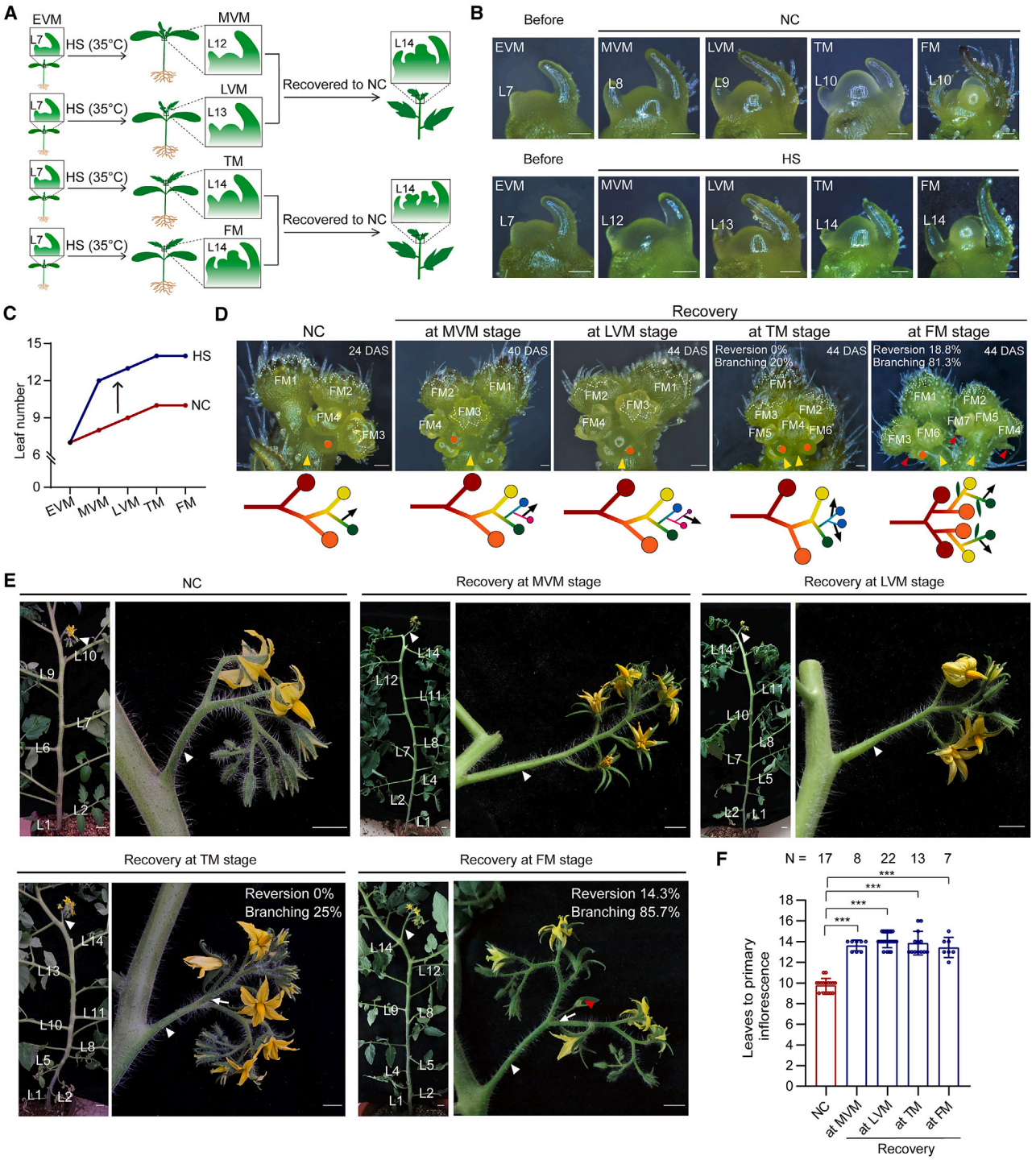

Figure 1. Reprogramming of SAM maturation at early vegetative meristem stage confers heat resilience in tomato

(A) Experimental design for heat treatment of tomato seedlings at EVM stage and recovery at different shoot apical meristem maturation stages.

(B and C) Stereoscope images (B) and leaf numbers of representative meristems (C) showing the SAM maturation process under HS. The numbers of meristems observed at different stages are 10, 10, 10, 10, and 32 for NC and 10, 10, 10, 10, and 65 for HS, respectively.

(D) Representative stereoscope images (upper) and schematics (bottom) showing the morphology of inflorescence meristems derived from primary shoot apex of WT plants under sustained NC or recovered from continuous HS when reaching the indicated stages. Yellow triangles indicate inflorescence branching. Orange dots indicate SIMs. Red triangles indicate vegetative reversions. The numbers of meristems used for the observation of inflorescence meristem architecture are 18, 8, 22, 10, and 16, respectively.

(legend continued on next page)

Please cite this article in press as: Huang et al., ROS burst prolongs transcriptional condensation to slow shoot apical meristem maturation and achieve heat-stress resilience in tomato, Developmental Cell (2025), https://doi.org/10.1016/j.devcel.2025.03.007

transcriptional condensates of TMF enable precise control of meristem maturation and flowering transition in tomato.[18] The biomolecular condensates formed by protein phase separation have been found to play critical roles in stress responses in various organisms.[20–22] The formation and maintenance of biomolecular condensates have been recently reported to be closely related to altered ROS levels.[18,23–25] As inevitable byproducts of cellular activity and energy metabolism, how ROS reprogram plant developmental processes through regulating protein phase separation to adapt to environmental changes has been a fundamental yet unresolved scientific question.

As one of the highest value fruit/vegetable crop worldwide, tomato originates from a relatively cool region in the Andes of South America (optimum growth temperature 22°C to 28°C) and is vulnerable to higher temperatures.[26–28] Tomato plants exhibit a sympodial growth habit and multiflowered inflorescences with a zigzag branching pattern.[29,30] The SAM maintains vegetative development before transitioning to reproductive development and terminating in an inflorescence meristem. The continuous growth of tomato plants arises from sympodial shoot meristems (SYMs), specialized axillary meristems that develop in the axil of the last leaf produced by the primary shoot meristem (PSM) and canonical axillary meristems.[29,31] The floral transition of tomato plants occurs after a stepwise SAM maturation program that can be developmentally defined and morphologically observed after removing the young leaves surrounding SAM,[18,29] making it an ideal model for exploring SAM development under stresses. Here, we find that heat-induced ROS facilitate the formation of TMF transcriptional condensates, which temporarily slows the SAM maturation process toward the reproductive state. This redox regulatory mechanism, a discovery in the molecular basis of developmental plasticity, allows tomato plants to prolong their vegetative growth as a coping mechanism under HS to maintain and optimize reproductive success.

RESULTS

Tomato plants slow SAM maturation to achieve heat-stress resilience

To explore whether and how SAM maturation responds to HS in tomato, we applied a 24-day continuous heat treatment using tomato cultivar Ailsa Craig (AC, WT) and monitored the developmental consequences during the entire SAM maturation process. Specifically, we transferred plants at an early vegetative meristem (EVM) stage from 26°C (normal condition, NC) to 35°C (HS) for continuous growth (Figure 1A) and analyzed the developmental differences between NC and HS at different SAM maturation stages, including middle vegetative meristem (MVM), late vegetative meristem (LVM), transition meristem (TM), and flower meristem (FM) stages. According to the plastochron index, the time interval between two successive leaf or flower primordia initiations during SAM development[32] and related morphological characteristics, the number of leaves, and the morphology of PSM are primary indicators of the maturation process.[29] Typically, every new leaf production marks a stage transition up to the TM.

For plants grown under NC, we observed a typically programmed maturation process as previously described (Figure 1B).[29] In contrast, heat-stress-treated plants dramatically delayed the transition from the EVM to the MVM stage, indicated by the production of around four more extra leaves (Figures 1B and 1C). Once the maturation process entered into the MVM stage, the interval of leaf numbers between different stages no longer showed differences between plants under NC and HS (Figures 1B and 1C). Finally, the plants suffering from HS produced four more leaves than under NC at flowering transition (Figures 1B and S1A). These results suggest that HS at the early vegetative stage of meristem maturation delays floral transition and the delay is mainly due to the longer duration of the vegetative meristem stage (Figure S1B).

We subsequently investigated the phenotypic outcomes of HS. As shown in Figure 1A, the aforementioned plants were allowed to grow until MVM, LVM, TM, and FM stages and then were moved to NC for recovery growth, respectively. Plants recovered at vegetative stages (MVM and LVM) showed normal inflorescence meristems (Figure 1D) and thus inflorescence architecture (Figure 1E). However, occasional branching began to appear on the PSM of plants recovered at TM stage, and much more frequent branching, along with a few vegetative reversions, occurred in the PSM of plants recovered at FM stage (Figure 1D), suggesting that HS alters the developmental fate of SAM once it enters the reproductive stage. Accordingly, despite the delay in flowering (Figures 1E and 1F), the primary inflorescences (the first inflorescence of the plant) of plants recovered at vegetative stages showed normal inflorescence architecture (Figure 1E). In contrast, the primary inflorescences of plants recovered at TM and FM stages showed branches, and vegetative reversions occurred in the primary inflorescences of plants recovered at FM stage (Figure 1E). Moreover, the fruit setting rate and yield of plants recovered at FM stage decreased 22.7% and 31.1%, respectively (Figures S1C–S1E). These results suggest that, if HS is stopped before the transitional stage (TM) of meristem maturation, plants only delay flowering transition by producing four extra leaves without significant reproductive development disruption and losses in fruit yield. However, if HS persists until the flowering transition stage (FM), it will lead to severe reproductive organ developmental defects and substantial yield losses. Therefore, we hypothesized that tomato plants prolong vegetative growth when experiencing HS at the vegetative meristem stage and prevent reproductive development from being exposed to HS to achieve heat resilience.

(E and F) Representative shoots and primary inflorescences (E) and quantification of flowering time (F) for WT plants under sustained NC or recovered from continuous HS when reaching the indicated stages. White triangles indicate inflorescences, white arrowheads indicate branching on inflorescences, and red triangles indicate vegetative reversions on inflorescences.

N, number of samples for quantification. Data are means ± SD, $^{***}p < 0.001$, Student's t test. NC, normal condition; HS, heat stress; EVM, early vegetative meristem; MVM, middle vegetative meristem; LVM, late vegetative meristem; TM, transition meristem; FM, flower meristem; L, leaf; DAS, day after sowing. Scale bars, 100 μm (B and D), 2 cm (E, plants), 1 cm (E, inflorescences).

See also Figure S1 and Table S2.

Please cite this article in press as: Huang et al., ROS burst prolongs transcriptional condensation to slow shoot apical meristem maturation and achieve heat-stress resilience in tomato, Developmental Cell (2025), https://doi.org/10.1016/j.devcel.2025.03.007

SAM maturation delay occurs at EVM stage in response to HS

To test the hypothesis, we performed stage-specific heat-stress treatments. Specifically, we grew tomato seedlings under NC until different SAM developmental stages, including EVM, MVM, LVM, TM, and FM stages. Subsequently, we simultaneously transferred plants at each aforementioned stage to 35°C for 14 days (Figure 2A). Compared with plants continuously grown under NC, the initiation and development of FM and sympodial inflorescence meristem (SIM), a specialized meristem formed within the inflorescence that produces another SIM on its side before terminating in a FM,[29,30] were severely repressed by HS (Figures 2B and S2A). After 14 days, the SAMs of plants grown under NC had reached the reproductive stage, with four to seven FMs and SIMs, displaying the normal "zigzag" inflorescence architecture (Figures 2B and S2A). Plants exposed to HS at EVM stage showed delayed meristem maturation, with a prolonged duration of vegetative meristem, entering the MVM and TM stages with the production of about four more leaves (Figures 2B and S2B). However, plants exposed to HS at other older stages (MVM, LVM, TM, and FM) produced the same number of leaves before flowering transition as the plants grown under NC (Figures 2B and S2B). Their FM and SIM developments were dramatically affected in these plants, seen in reduced production of floral primordia, occurrence of vegetative reversions, and increased branching events on inflorescence meristems (Figures 2B and S2A). These results suggest that HS perturbs the programmed development of SAM and triggers reprogramming in certain cases.

To assess the phenotypic consequences of the 14-day heat-stress treatment, we analyzed phenotypes of mature plants that were transferred to NC for recovery growth after heat treatment. Despite EVM-stage plants producing four more leaves at flowering transition after heat treatment, they developed normal inflorescence architecture and floral organs (Figures 2C and 2D). Consequently, the fruit setting and yield of the primary inflorescences in these plants were not affected by HS (Figures 2E–2G). In contrast, plants subjected to HS at older stages (MVM, LVM, TM, and FM) did not show changes in leaf number at flowering transition, but their primary inflorescences exhibited frequent branches and vegetative reversions (Figures 2C and 2D). Specifically, aborted flowers were frequently observed on the primary inflorescences in plants treated at TM and FM stages, with the even-higher severity of flower abortion in plants treated at FM stage (Figure 2C), suggesting that HS occurring during reproductive stages exacerbates the severity of the effects. These floral development defects caused significantly decreased fruit setting with a lost fruit yield of approximately 39.8%, 33.6%, 35%, and 63% in plants heat-treated at MVM, LVM, TM, and FM stages, respectively (Figures 2E–2G). These results indicate that tomato plants actively reprogram shoot meristem maturation in response to HS by delaying the maturation process and extending the vegetative state to mitigate stress damage, and this adaptive response occurs at the EVM stage.

The heat-responsive delay of SAM maturation relies on ROS burst

Next, we explored the signal that reprograms the meristem maturation. Given that ROS burst is a hallmark of environmental stress responses in plants, it might be utilized as the signal to reprogram SAM maturation in response to HS. There are various pathways for ROS metabolism in organisms. Among them, respiratory burst oxidase homologs (RBOHs) catalyze the conversion of O_2 to $O_2^{\cdot-}$, which is then rapidly converted into H_2O_2 by superoxide dismutases (SODs). Subsequently, H_2O_2 is reduced to H_2O by various systems, including peroxiredoxin (PRX)/thioredoxin (TRX), glutathione peroxidase (GPX)/glutathione (GSH), and catalase (CAT) (Figure 3A).[17,33–35] Loss of *SlRBOH1* and *SlRBOH2*, two *RBOH* genes that are highly expressed in tomato SAM, accelerated SAM maturation and promoted early flowering.[18] We then analyzed the phenotypic changes of the *RBOH*-deficient tomato mutant upon HS by applying the heat treatment to the seedlings at the EVM stage. To rapidly examine ROS levels in living plants, we used the nonfluorescent dye 3,3′-diaminobenzidine (DAB) (Figure S3A) and nitroblue tetrazolium (NBT) staining to detect H_2O_2 and $O_2^{\cdot-}$, respectively (Figure S3C). We observed lower ROS levels in the leaves of *Slrboh1 Slrboh2* mutant plants than those of wild type (WT) under NC (Figures S3A–S3D). To accurately monitor ROS levels in SAMs, we used a more sensitive fluorescent probe of ROS, hydroxyphenyl fluorescein (HPF). HPF staining indicated decreased ROS levels in leaves of *Slrboh1 Slrboh2* mutant (Figures S3E and S3F), resembling the results of DAB and NBT staining. HS strongly induced ROS accumulation in SAMs of WT plants but not in those of *Slrboh1 Slrboh2* mutant plants (Figures 3B and 3C), indicating that heat-stress-induced ROS accumulation is impaired in the *Slrboh1 Slrboh2* plants.

We then tracked the SAM maturation in the WT and *Slrboh1 Slrboh2* plants that were treated at EVM stage with continuous HS. In contrast to meristem maturation delay observed in WT plants, the *Slrboh1 Slrboh2* mutant plants produced the same number of leaves at flowering transition as observed under NC (Figures 3D and 3E), suggesting that the *Slrboh1 Slrboh2* plants are unable to reprogram the meristem maturation for stress adaption (Figure 3F). Specifically, heat-treated *Slrboh1 Slrboh2* plants progressed to the FM stage whereas WT plants remained in the vegetative meristem stage due to the heat-induced delay of meristem maturation (Figure 3F). To investigate whether the heat-induced delay is dependent on the developmental stage of the meristem when experiencing stress or the absolute age of the plant (indicated by the number of leaves), we conducted heat treatment on WT and *Slrboh1 Slrboh2* mutant plants that had the same number of leaves but were at different developmental stages of the meristem. Specifically, WT plants are at the EVM stage after producing seven leaves, whereas the *Slrboh1 Slrboh2* mutant is already at the MVM stage when producing seven leaves due to its slight early-flowering phenotype.[18] The results indicated that the WT showed an expected meristem maturation delay, with production of about four more leaves at flowering transition under HS, whereas *Slrboh1 Slrboh2* mutant plants exhibited the same number of leaves at flowering transition as they did under NC (Figures S3G and S3H), suggesting that heat-responsive delay is linked to the developmental stage of plants rather than their age. To investigate the phenotypic consequences of mature plants, we simultaneously transferred the heat-treated WT and *Slrboh1 Slrboh2* plants to NC for recovery growth. In contrast to WT plants that produced normal inflorescence architecture and floral organs (Figures 3G and 3H), *Slrboh1 Slrboh2* plants showed

Please cite this article in press as: Huang et al., ROS burst prolongs transcriptional condensation to slow shoot apical meristem maturation and achieve heat-stress resilience in tomato, Developmental Cell (2025), https://doi.org/10.1016/j.devcel.2025.03.007

CellPress
OPEN ACCESS

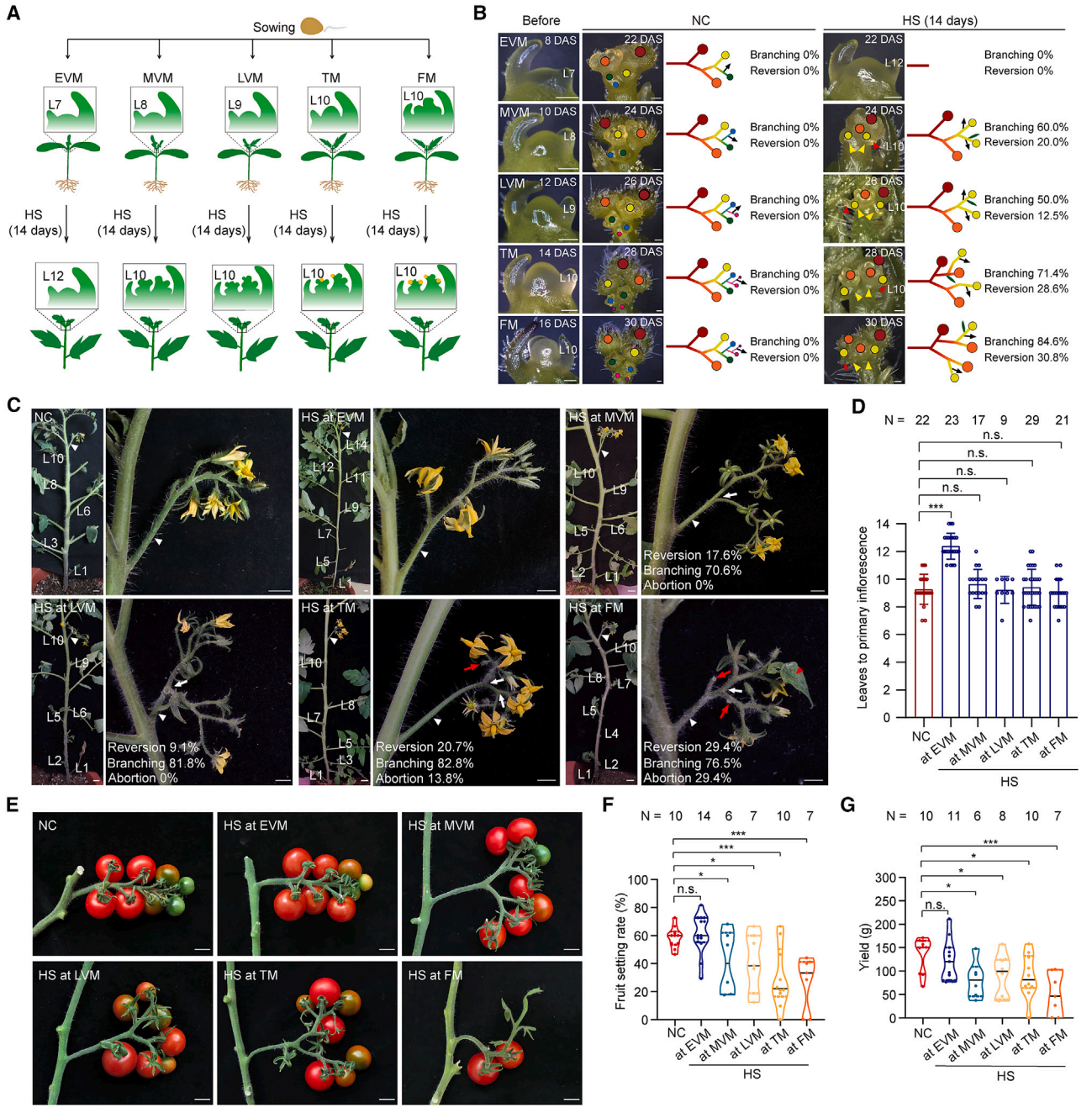

Figure 2. Developmental and fruit yield consequences of heat stress on tomato seedlings at different SAM maturation stages

(A and B) Experimental setup (A) and representative stereoscope images and schematics showing the effects of 14-day HS on shoot apical meristem at different stages (B). DAS, day after sowing. The numbers of meristems used for quantification are 8, 6, 10, 8, and 8 for NC and 8, 5, 8, 7, and 13 for HS, respectively. The colored dots (red, orange, yellow, green, blue, pink, and purple dots) indicate SIMs and FMs. Red triangles indicate vegetative reversions, and yellow triangles indicate branching events. Green ovals indicate vegetative reversions.

(C and D) Representative images of plant and primary inflorescence (C) and quantification of leaves at flowering (D) for plants recovered to NC after 14-day HS treatment at different SAM maturation stages. White triangles indicate primary inflorescences, white arrowheads indicate branching, red triangles indicate vegetative reversions, red arrowheads indicate aborted flowers.

(E–G) Representative images of fruits (E), quantification of fruit setting rate (F) and yield (G) for the primary inflorescences of plants recovered from 14-day HS at different developmental stages.

N, number of samples for quantification. Data are means ± SD, $*p < 0.05$, $***p < 0.001$, Student's t test. n.s., not significant; NC, normal condition; HS, heat stress; EVM, early vegetative meristem; MVM, middle vegetative meristem; LVM, late vegetative meristem; TM, transition meristem; FM, flower meristem; L, leaf. Scale bars, 100 μm (B), 2 cm (C, plants; E), and 1 cm (C, inflorescences).

See also Figure S2 and Table S2.

Please cite this article in press as: Huang et al., ROS burst prolongs transcriptional condensation to slow shoot apical meristem maturation and achieve heat-stress resilience in tomato, Developmental Cell (2025), https://doi.org/10.1016/j.devcel.2025.03.007

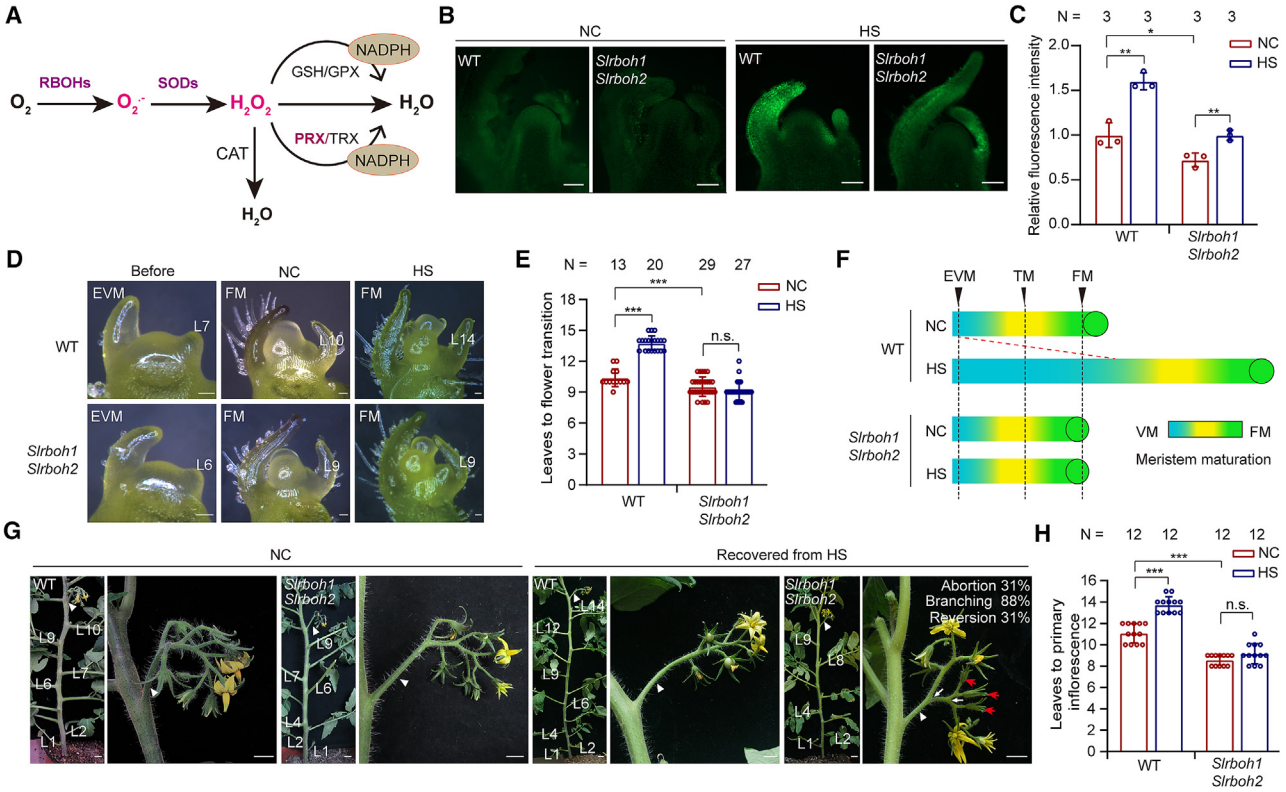

Figure 3. The delay of flowering transition relies on heat-induced H_2O_2 accumulation

(A) Schematic diagram of ROS metabolism in plants.

(B and C) Representative images (B) and intensity quantification (C) of HPF staining showing ROS level in the meristems of WT and *Slrboh1 Slrboh2* mutants under NC and HS.

(D–F) Stereoscope images (D), quantification of leaves at flower transition (E), and schematic diagram (F) showing the SAM maturation process of WT and *Slrboh1 Slrboh2* under NC and HS.

(G and H) Representative shoots and primary inflorescences (G) and quantification data (H) of flowering time for WT and *Slrboh1 Slrboh2* mutant plants grown under NC and recovered from continuous HS when *Slrboh1 Slrboh2* mutant plants reached FM, respectively. White triangles indicate primary inflorescences, white arrowheads indicate branching, red arrowheads indicate aborted flowers.

N, number of samples for quantification. Data are means ± SD, $*p < 0.05$, $**p < 0.01$, $***p < 0.001$, Student's t test. n.s., not significant; NC, normal condition; HS, heat stress; EVM, early vegetative meristem; VM, vegetative meristem; TM, transition meristem; FM, flower meristem; L, leaf. Scale bars, 100 μm (B), 50 μm (D), 2 cm (G, plants), and 1 cm (G, inflorescences).

See also Figure S3 and Table S2.

disordered reproductive development. Specifically, their inflorescences showed 88% branching and 31% reversion events, accompanied by a frequent occurrence of aborted flowers (Figures 3G and 3H). The fruit setting rate and fruit yield were comparable between WT and *Slrboh1 Slrboh2* plants under NC (Figures S3I and S3J). However, the *Slrboh1 Slrboh2* plants exhibited a significant decline in both traits when subjected to HS. Specifically, the fruit setting rate decreased by 59.37% and the fruit yield decreased by 57.4% in *Slrboh1 Slrboh2* plants (Figures S3I and S3J). These results suggested that heat-induced accumulation of ROS protects SAM maturation from precocious exposure of reproductive organs to stress damage.

HS reprograms meristem maturation through TMF

TMF acts as a transcriptional switch for flowering transition in tomato by sensing developmentally produced ROS and forming transcriptional condensates via protein phase separation.[18,36] We applied heat treatment to *tmf* mutants to investigate whether heat-stress-induced delay of SAM maturation relies on TMF. The results showed that the *TMF* null mutant, *tmf-1*, failed to delay SAM maturation in response to HS (Figures S4A and S4B). Given that *tmf-1* shows strong phenotypes in flowering time and inflorescence architecture due to rapidly precocious termination of meristem maturation,[36] we therefore confirmed the effects by taking advantage of the *tmf-2* mutant. This allele displays a more moderate effect, resulting in the flowering of approximately two leaves earlier than the WT.[36] Likewise, we found that *tmf-2* plants did not delay meristem maturation marked by producing extra leaves, as seen in WT plants (Figures 4A–4C). Notably, the heat-induced accumulation of ROS in the *tmf* mutants was found to be indistinguishable from that in WT plants, thereby excluding any phenotypic influences arising from changes in ROS levels (Figures S4C–S4F). The *tmf-2* mutant plants showed a high frequency of branching (57%) on the primary inflorescences along with aborted flowers (Figures 4D and 4E), resembling the effects observed in the ROS production-deficient

Please cite this article in press as: Huang et al., ROS burst prolongs transcriptional condensation to slow shoot apical meristem maturation and achieve heat-stress resilience in tomato, Developmental Cell (2025), https://doi.org/10.1016/j.devcel.2025.03.007

CellPress
OPEN ACCESS

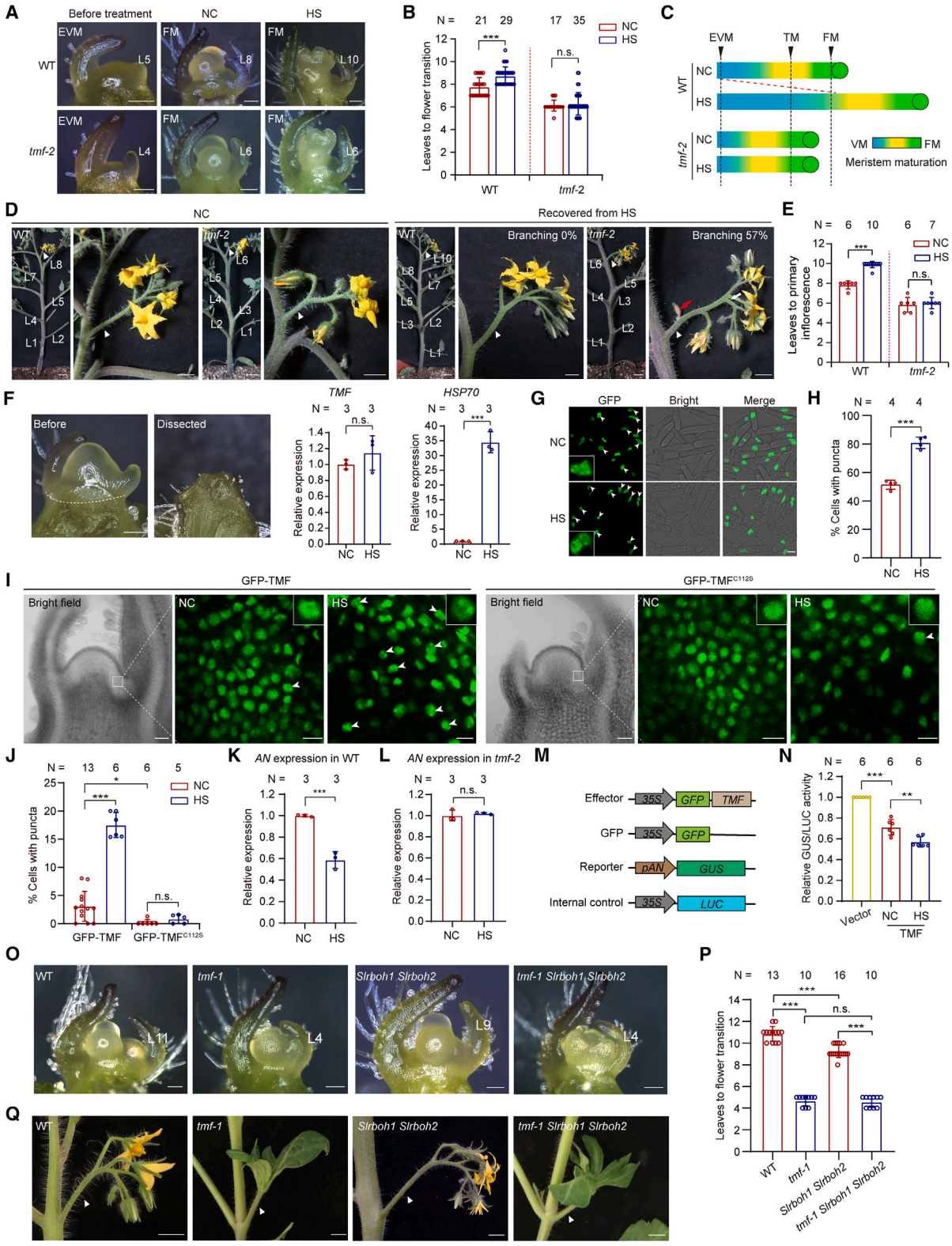

Figure 4. HS slows flowering transition through extending transcriptional condensation of TMF protein

(A–C) Stereoscope images (A), quantification of leaves at flower transition (B), and schematic diagram (C) showing the SAM maturation process of WT and *tmf-2* plants under NC and HS.

(legend continued on next page)

Please cite this article in press as: Huang et al., ROS burst prolongs transcriptional condensation to slow shoot apical meristem maturation and achieve heat-stress resilience in tomato, Developmental Cell (2025), https://doi.org/10.1016/j.devcel.2025.03.007

Slrobh1 Slrobh2 mutant (Figure 3G). Moreover, the overexpression of TMF resulted in a slight delay in the flowering transition, with approximately two additional leaves compared with WT under NC (Figures S4G and S4H). This delay was further exacerbated by HS, with an additional increase of approximately two leaves (Figures S4G and S4H). Collectively, these results indicate that the heat-stress-responsive delay of SAM maturation is dependent on TMF.

ROS burst prolongs transcriptional repression status of TMF condensates

We next investigated how heat-induced ROS slow meristem maturation for stress resilience. Given that HS did not change the transcription level of *TMF* (Figure 4F), we hypothesized that the regulatory mechanism may reside in the stress-responsive control of TMF protein behavior. To test this, we examined status changes of TMF condensates in living cells. We took advantage of a fission yeast system that is widely used for investigating protein phase separation in both animals and plants.[37–40] When expressed in fission yeast cells, the GFP-TMF protein showed a typical punctate localization in the nucleus, similar to the pattern in the cells of tomato plants (Figure 4G).[18] Heat treatment significantly enhanced the formation of TMF condensates (Figures 4G and 4H). To validate this *in planta*, we subjected the GFP-TMF transgenic tomato plants to heat-stress treatment and observed TMF condensates. Heat treatment led to a significant enhancement in TMF condensation, characterized by approximately a 20-fold increase in the proportion of punctate-localized GFP-TMF protein in the nucleus compared with NC (Figures S4I and S4J). This phenomenon is reminiscent of the changes in TMF condensates induced by ROS application.[18] We then explored whether the changes of TMF phase separation status rely on endogenous ROS levels. We expressed GFP-TMF in the WT and *Slrboh1 Slrboh2* mutant with reduced ROS levels (Figures 3B, 3C, and S3A–S3F) and found that the proportion of cells with punctate-localized GFP-TMF was significantly reduced by approximately 46% in the *Slrboh1 Slrboh2* mutant compared with WT (Figures S4K and S4L). These results suggest that heat-stress-induced TMF condensation depends on cellular ROS accumulation.

Cysteine residues at positions 112, 124, and 126 of the TMF protein can sense and become oxidized by cellular ROS, resulting in the formation of intermolecular and intramolecular disulfide bonds that drive protein phase separation.[18] To test whether the enhanced TMF protein phase separation is caused by the sensing of heat-stress-induced ROS, we mutated the cysteine at position 112 to serine (GFP-TMF^{C112S}) and examined the phase separation property by transiently expressing in tobacco plants. In contrast to the noticeably heat-responsive increase in puncta formation observed in the GFP-TMF protein, the status of the GFP-TMF^{C112S} variant showed a slight change under HS (Figures S4M and S4N). To validate this in living tomato plants, we generated complementation transgenic plants in the *tmf* mutant by expressing GFP-TMF and GFP-TMF^{C112S}, respectively. Expression of GFP-TMF rescued the early flowering and single-flower phenotypes of *tmf* mutant plants as described previously, suggesting a normal function of TMF.[18,36] We examined changes in the phase separation status of GFP-TMF and GFP-TMF^{C112S} in response to HS within the SAM. HS dramatically increased the proportion of GFP-TMF condensates in the shoot apical stem cells (Figures 4I and 4J). However, the GFP-TMF^{C112S} protein did not show such responsive changes (Figures 4I and 4J). Consistently, GFP-TMF^{C112S} could not rescue the phenotype of *tmf* mutant plants.[18] These results suggest that stress-responsive enhancement of TMF protein phase separation relies on sensing of heat-induced ROS.

We next explored how heat-induced TMF condensation affects gene expression. We previously reported that TMF directly binds the promoter of the floral identity gene *ANANTHA* (*AN*) to repress its expression until the onset of flowering transition.[18] Activation of *AN* marks initiation of floral transition in tomato plants. We performed microdissection of the TMs for reverse-transcriptase quantitative PCR (RT-qPCR) analysis and found that HS delayed the transcriptional activation of *AN* in the SAMs of WT plants (Figure 4K). In contrast, the *AN* expression in the *tmf-2* mutant showed no significant difference between NC and HS (Figure 4L), suggesting that TMF-controlled *AN* expression underlies the delay of meristem maturation caused by HS. To test the direct transcriptional regulation of TMF on *AN* under HS, we performed GUS-LUC dual reporter assays in tobacco plants (Figure 4M). We found that the degree of transcriptional repression of *AN*'s expression was associated with the enhancement of TMF condensate formation under HS (Figure 4N). To genetically test whether ROS-burst-controlled heat resilience relies on TMF, we crossed *tmf-1* with *Slrboh1 Slrboh2*

(D and E) Representative shoots and primary inflorescences (D) and quantification data (E) of flowering time for WT and *tmf-2* mutant plants grown under NC and recovered from continuous HS when *tmf-2* reached FM stage, respectively. White triangles indicate primary inflorescences, white arrowheads indicate branching, red arrowheads indicate aborted flowers.

(F) Representative image of micro-dissected transitional meristems (left) for real-time PCR analysis. Relative expression was normalized to the expression under NC. *UBIQUITIN* (*UBI*) and *HSP70* serve as an internal control and positive control, respectively.

(G and H) Representative images (G) and quantification data (H) showing enhanced protein phase separation of TMF under HS in yeast cells. White arrowheads indicate nuclei with puncta.

(I and J) Representative images (I) and quantification data (J) of nuclei with puncta in the SAM of transgenic plants expressing GFP-TMF and GFP-TMF^{C112S} in *tmf* mutant under NC and HS, respectively. White arrowheads indicate nuclei with puncta.

(K and L) Relative expression of *AN* in the transitional meristems of WT (K) and *tmf-2* mutant (L) under HS. *UBI* served as an internal control.

(M and N) Schematics of constructs (M) and transcriptional repression of *AN* under HS (N). The ratio of GUS/LUC was used to indicate the relative transcriptional activity, using LUC as an internal control.

(O–Q) Representative stereoscope images of meristems (O), quantification of leaves at flower transition (P), and representative primary inflorescences (Q) for WT, *tmf-1*, *Slrboh1 Slrboh2*, and *tmf-1 Slrboh1 Slrboh2*. White triangles indicate primary inflorescences.

N, number of samples for quantification. Data are means ± SD, $^{*}p < 0.05$, $^{**}p < 0.01$, $^{***}p < 0.001$, Student's t test. n.s., not significant; NC, normal condition; HS, heat stress; EVM, early vegetative meristem; VM, vegetative meristem; TM, transition meristem; FM, flower meristem; L, leaf. Scale bars, 100 μm (A and O), 2 cm (D, plants), 1 cm (D, inflorescences; Q), 5 μm (G), 50 μm (I, bright), and 10 μm (I, GFP).

See also Figure S4 and Table S2.

Please cite this article in press as: Huang et al., ROS burst prolongs transcriptional condensation to slow shoot apical meristem maturation and achieve heat-stress resilience in tomato, Developmental Cell (2025), https://doi.org/10.1016/j.devcel.2025.03.007

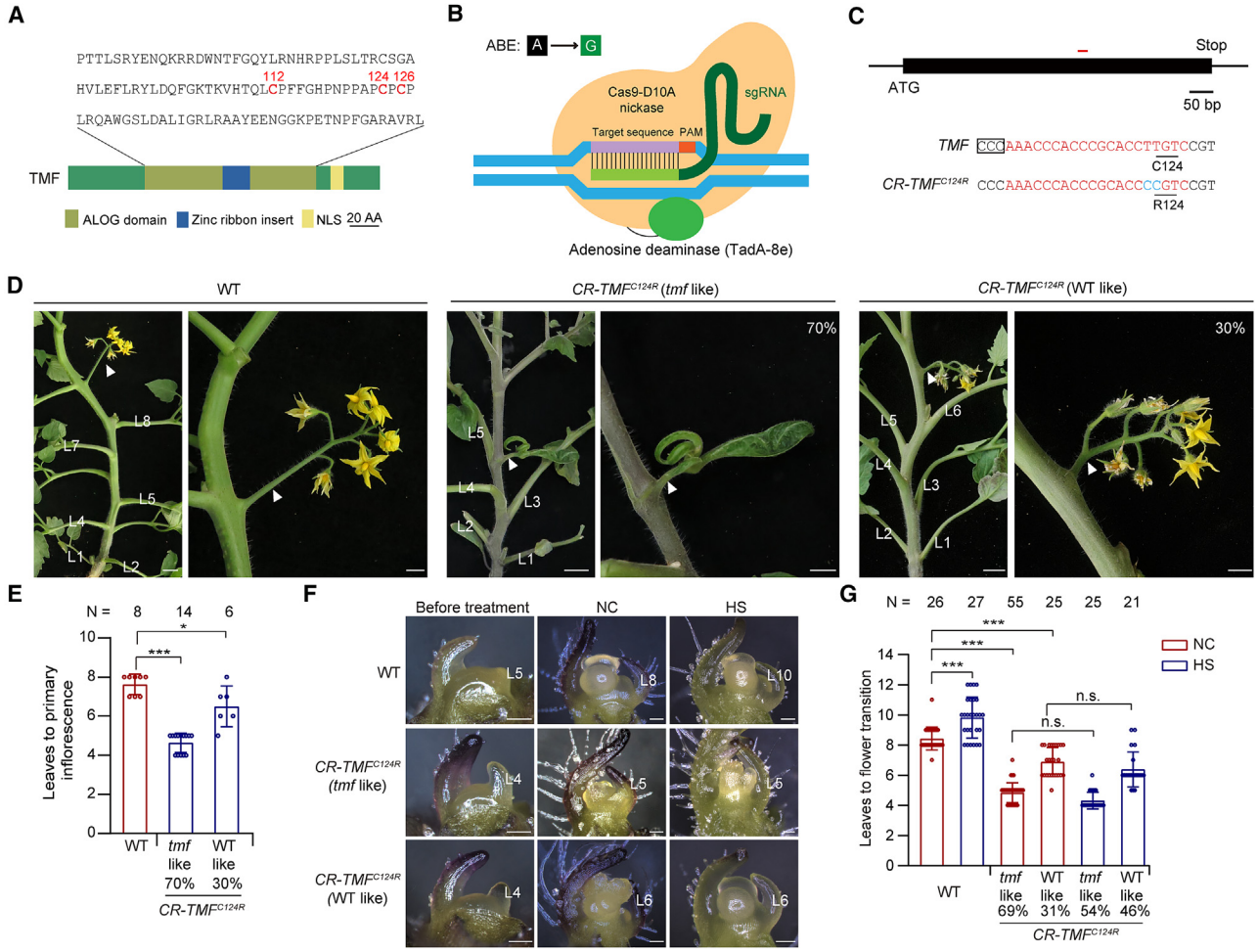

Figure 5. Base editing of H_2O_2-sensing cysteine residue of TMF abolishes heat-stress resilience of meristem maturation

(A) Schematic of TMF protein domains and amino acid sequence of the ALOG domain. Conserved cysteine residues for disulfide bond formation are shown in red. NLS, nuclear localization signal.

(B) Schematic diagram of adenine base editor (ABE). sgRNA, single guide RNA; PAM, protospacer adjacent motif; A, adenine; G, guanine.

(C) Schematic indicating sgRNA (red line, upper) and allelic information (bottom) for *CR-TMF*^{C124R}.

(D and E) Representative shoots and primary inflorescences (D) and quantification of flowering time (E) for WT and *CR-TMF*^{C124R} mutants grown under NC. We refer to the ~70% of *CR-TMF*^{C124R} mutant plants with single-flowered primary inflorescences as *CR-TMF*^{C124R} (*tmf*-like) and the remaining ~30% of plants with multiple-flowered primary inflorescences as *CR-TMF*^{C124R} (WT-like). White triangles indicate primary inflorescences.

(F and G) Stereoscope images (F) and quantification of leaves at flower transition (G) in WT and *CR-TMF*^{C124R} mutants under NC and HS.

N, number of samples for quantification. Data are means ± SD, $*p < 0.05$, $***p < 0.001$, Student's t test. n.s., not significant; NC, normal condition; HS, heat stress; L, leaf. Scale bars, 2 cm (D, plants), 1 cm (D, inflorescences), and 100 μm (F).

See also Figure S5 and Table S2.

and generated *tmf-1 Slrboh1 Slrboh2* triple mutant. The resulting phenotypes of the *tmf-1 Slrboh1 Slrboh2* mutant in terms of SAM maturation, flowering time, and inflorescence architecture were indistinguishable from those observed in the *tmf-1* single mutant (Figures 4O–4Q), suggesting that *TMF* is epistatic to *SlRBOH1* and *SlRBOH2*. Together, these results demonstrated that TMF is the executor of the meristem maturation delay induced by the ROS burst.

Base editing of endogenous TMF transcriptional condensates abolishes stress resilience

Despite the evidence generated by overexpression and complementary transgenic plants, the spatiotemporal property of TMF expression and condensation, as well as fine-scale localization of ROS signals, makes endogenous mutation of TMF the ideal strategy to investigate its phase separation behavior *in vivo*. TMF contains an ALOG domain with three functional conserved cysteine residues—C112, C124, and C126—that sense ROS to form disulfide bonds and trigger phase separation (Figure 5A).[18] Expression of GFP-TMF^{C112S} could not rescue the *tmf* mutant phenotypes, establishing the function of cysteine-mediated protein phase separation for TMF.[18] To precisely alter the endogenous cysteine residues of TMF, we took advantage of the adenine base editor (ABE), which efficiently generates adenine (A)-to-guanine (G) conversion and is composed of a nickase-type Cas9 (nCas9) and an adenosine deaminase (Figure 5B).[41]

Please cite this article in press as: Huang et al., ROS burst prolongs transcriptional condensation to slow shoot apical meristem maturation and achieve heat-stress resilience in tomato, Developmental Cell (2025), https://doi.org/10.1016/j.devcel.2025.03.007

We generated a vector *pDIRECT-22C-ABE8e* containing the genes that encode the evolved adenosine deaminase TadA-8e of *Escherichia coli* and nCas9, respectively.[42,43] Due to the limits imposed by editing windows and features of the ABE system, only two target sites were available over the three cysteine residues, one for C124 and one for C126. Fortunately, one of them allowed us to successfully generate a *CR-TMF*^{C124R} mutant, encoding a TMF variant with C124 changed to R124 (Figure 5C). Compared with WT, the *CR-TMF*^{C124R} mutant plants displayed early flowering and a single flower with magnified leaf-like sepals in the primary inflorescences, and the phenotype of the single flower showed about 70% penetrance (Figures 5D and 5E).[44] Specifically, we referred to these *CR-TMF*^{C124R} mutant plants as *CR-TMF*^{C124R} (*tmf*-like) and the ~30% remaining plants as *CR-TMF*^{C124R} (WT-like), as they only showed early flowering but not the single-flower phenotype due to the penetrance (Figures 5D and 5E). The phenotypes of the *CR-TMF*^{C124R} mutant were similar to the classic *tmf* mutant,[36] suggesting that the C124R mutation disrupted TMF biological function. Consistently, TMF^{C124R} proteins exhibited a nearly complete loss of phase separation capacity (Figure S5).

We next investigated phenotypes of *CR-TMF*^{C124R} mutant plants under HS. We applied a continuous HS treatment to WT and *CR-TMF*^{C124R} mutant plants at EVM stage. Under NC, the *CR-TMF*^{C124R} mutant showed precocious SAM maturation and early flowering, as mentioned before (Figures 5F and 5G). However, the meristem maturation delay did not occur in the *CR-TMF*^{C124R} mutant plants after heat treatment (Figures 5F and 5G), resembling the phenotypes of *tmf-1* and *tmf-2* mutants and the ROS-production-deficient mutant *Slrboh1 Slrboh2*. Together, these findings provide compelling genetic evidence that ROS-induced SAM maturation delay in response to HS is controlled by cysteine-residue-governed TMF transcriptional condensates.

Manipulation of endogenous ROS level confers plasticity of SAM maturation

ROS level often has such widespread pleiotropic effects on plant growth that it becomes difficult to focus on when studying any specific phenotype or trait. Here, the demonstration of TMF function provided us with a rare opportunity to fine-tune the ROS level, as well as a gene's response, to reprogram the developmental process in a precise spatiotemporal context. To achieve this, we used the *TMF* promoter, which is predominantly active in vegetative meristems,[36] to specifically express *SlRBOH1* to enhance ROS production. The resulting *pTMF:SlRBOH1-YFP* transgenic plants showed slower meristem maturation, indicated by producing approximately two more leaves at the floral transition compared with WT plants (Figures 6A and 6B). Accordingly, the flowering time of mature plants was also delayed by approximately two leaves (Figures 6C and 6D). These results suggest that manipulating ROS level by tweaking enzymes in the ROS-generating pathway in a precise spatiotemporal context can reprogram meristem maturation and flowering.

We subsequently tuned down the activity of the ROS-scavenging pathway by engineering peroxidases that express in SAM and putatively catalyze the reduction of H_2O_2 into H_2O. This intervention was expected to lead to the accumulation of endogenous H_2O_2. We used CRISPR-Cas9 technology to knock out two tomato peroxidase genes that are highly expressed in SAMs: *Solyc01g108320* (designated as *SlPRX1*) and *Solyc12g096530* (designated as *SlPRX2*) (Figures S6A and S6B). Both genes are putative homologs of the Arabidopsis peroxidase *PRX69* (*AT5G64100*), which is specifically expressed in shoot apical stem cells to restrict H_2O_2 accumulation.[17] The H_2O_2 levels in the leaves of *CR-SlPRX1* and *CR-SlPRX2* mutants were significantly elevated, but the $O_2^{\cdot-}$ levels did not show significant difference from WT plants (Figures S6C–S6J), suggesting that loss of *SlPRX1* or *SlPRX2* induces ROS accumulation by reducing the conversion of H_2O_2 to H_2O. Both *CR-SlPRX* mutants exhibited a delay in SAM maturation and flowering transition compared with WT plants. Specifically, the *CR-SlPRX1* mutant produced approximately five more leaves before the transition to flowering (Figures S6K–S6N), whereas the *CR-SlPRX2* mutant exhibited a weaker phenotype, resulting in only two extra leaves prior to the flowering transition (Figures 6E–6H). These results suggest that the ROS accumulation achieved by partially blocking H_2O_2 catabolism mimics the ROS burst induced by HS, both of which similarly adjust plant architecture by reprogramming shoot apical stem cell maturation. The results suggest that dynamic changes of ROS levels enable developmental reprogramming and plasticity of plants. Manipulating ROS in such a fine spatial scale to adjust the SAM maturation program could serve as an effective means to preserve tomato productivity—and possibly that of other crops—in the face of environmental stresses.

DISCUSSION

Optimal SAM development is crucial for ensuring efficient and balanced growth of different plant organs, in particular the transition from vegetative to reproductive growth, which directly determines plant aerial architecture and yield.[29,45,46] As a result of angiosperm evolution, the development of the SAM is a sophisticatedly orchestrated process determined by various genetic and environmental factors.[47] Genetic factors determine the inherent growth program and architecture of the SAM,[29,48] whereas environmental factors influence the spatiotemporal manifest of the inherent program.[49,50] Plasticity, environmentally attuned developmental reprogramming, is an important mechanism that helps plants respond, adjust, and acclimate to various environmental stresses.[51,52] We demonstrated that cellular ROS control the programming and reprogramming of SAM development via TMF transcriptional condensates, enabling normal growth and heat resilience in tomato, respectively (Figure 6I). Under NC, the normal local ROS control SAM maturation and synchronize flowering through TMF transcriptional condensates. This process relies on cysteine-mediated formation of disulfide bonds (Figure 6I).[18] Under HS, accumulated ROS enhance the formation of TMF transcriptional condensates and prolong its transcriptional repression on the floral identity gene to extend vegetative growth of the SAM, preventing precocious transition to reproductive growth and avoiding damage to reproductive growth by stress, as continued HS during FM development results in flower abortion and yield loss (Figure 6I). The molecular links between HS, ROS, and TMF condensates established in this study provide us with an opportunity to devise genetic and environmental manipulations for tuning the SAM maturation process and thus the ability to develop crop varieties with improved stress tolerance and productivity.

Please cite this article in press as: Huang et al., ROS burst prolongs transcriptional condensation to slow shoot apical meristem maturation and achieve heat-stress resilience in tomato, Developmental Cell (2025), https://doi.org/10.1016/j.devcel.2025.03.007

CellPress
OPEN ACCESS

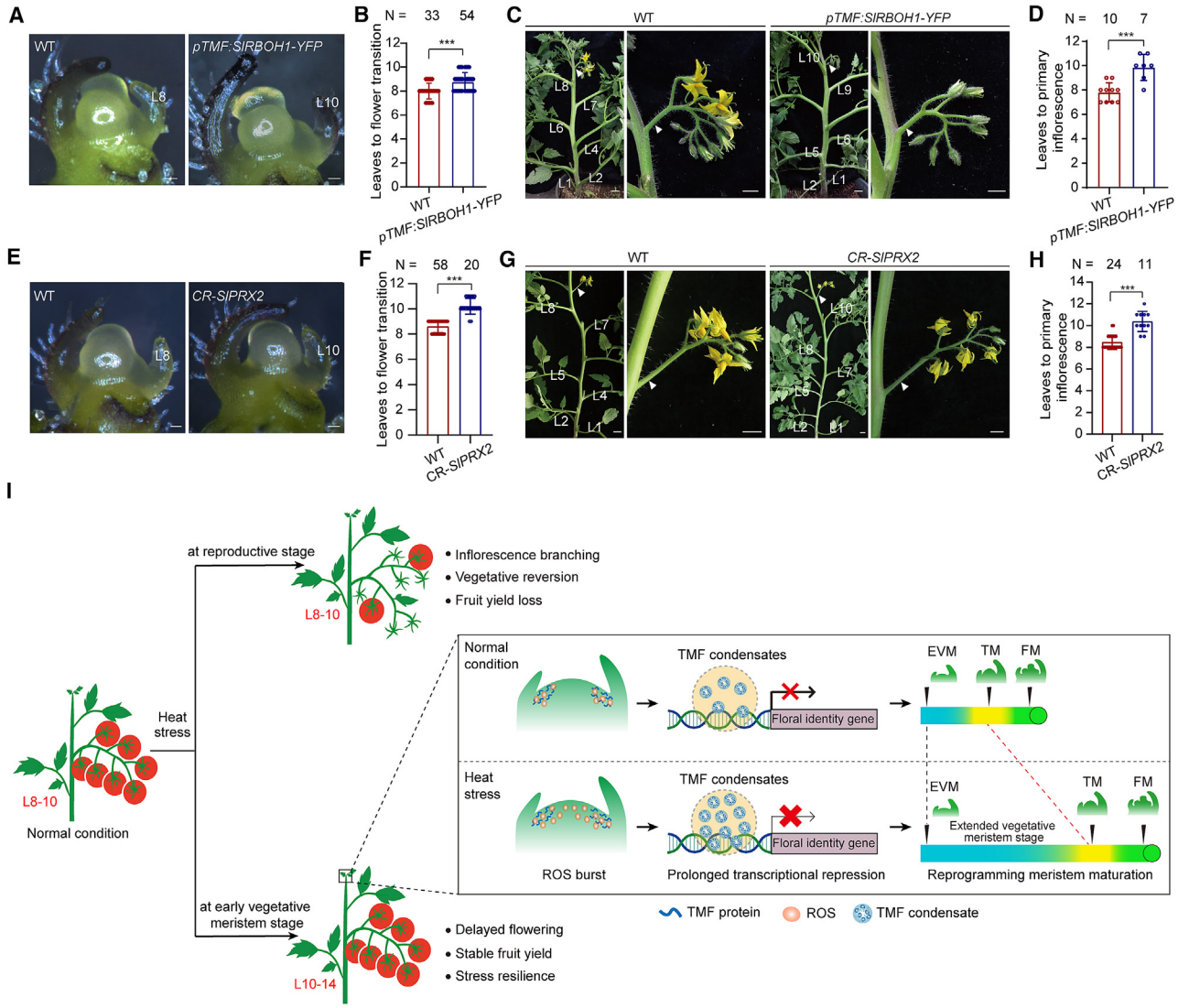

Figure 6. Manipulation of endogenous ROS level confers flowering plasticity in tomato

(A and B) Representative stereoscope images of meristems (A) and quantification of leaves at flower transition (B) for WT and *pTMF:SlRBOH1-YFP* transgenic plants.

(C and D) Representative shoots and primary inflorescences (C) and quantification of flowering time (D) for WT and *pTMF:SlRBOH1-YFP* transgenic plants. White triangles indicate primary inflorescences.

(E and F) Representative stereoscope images of meristems (E) and quantification data of leaves at flower transition (F) for WT and *CR-SlPRX2* mutant plants.

(G and H) Representative shoots and primary inflorescences (G) and flowering time quantification (H) for WT and *CR-SlPRX2* mutant plants. White triangles indicate primary inflorescences.

(I) A working model for TMF-controlled developmental plasticity and heat resilience in tomato. EVM, early vegetative meristem; TM, transition meristem; FM, flower meristem.

N, number of samples for quantification. Data are means ± SD, ***$p < 0.001$, Student's t test. n.s., not significant. NC, normal condition; HS, heat stress; L, leaf. Scale bars, 50 μm (A and E), 2 cm (C and G, plants), and 1 cm (C and G, inflorescences).

See also Figure S6 and Table S2.

This mechanism emphasizes the critical need for monitoring and controlling temperature during the seedling stage in agricultural practices. It guides farmers in making informed decisions by either adjusting sowing times or by precisely controlling seedling growth temperatures. Such measures are essential for balancing harvest timing and mitigating yield penalties caused by global warming.

ROS signaling is implicated in multiple biological processes in plants' responses to environmental changes. Our findings demonstrate that overproduced ROS contribute to the fine-tuning of SAM development for heat resilience by extending standby transcriptional condensates. Heat-induced ROS may act as a signal that triggers developmental plasticity in shoot apical stem cells, maintaining them in an undifferentiated and

pluripotent state in response to HS. This mechanism represents a redox-controlled bet-hedging strategy with which plants actively cope with HS, but it needs a molecular underpinning. Protein phase separation provides a dynamic and spatial framework for transcriptional regulation by organizing and compartmentalizing transcriptional molecules and facilitating their interaction. With signal-sensing ability and state/phase reversibility, protein phase separation is well-suited to serve as the molecular basis of precisely controlled developmental plasticity.[53] The formation of protein condensates is sensitive to environmental stresses, such as heat, cold, and osmotic stress.[37,54–56] ROS, serving as signals in stress responses, relay environmental signals and modify proteins by oxidizing critical residues, such as cysteine residues, which, in turn, alter their phase separation properties.[18,23,57] Cysteine exists in various forms, depending on the pH and redox environment, and this flexibility establishes it as an excellent candidate for controlling phase separation in biomolecular condensates involved in diverse biological processes. Our research demonstrates how plants achieve heat resilience through the precise coupling of ROS sensing with loci-specific transcriptional suppression via phase separation. This redox-controlled developmental reprogramming mechanism is not only the basis of this particular case of plant developmental plasticity but may also represent a more common strategy employed by biological systems to cope with variable environmental stresses. This mechanism sheds light on the genetic and molecular basis of developmental plasticity, a largely evolutionary puzzle, paving the way to exploit the mechanism to create more flexible, resilient, and adaptable crops.

Limitations of the study

The development of SAM occurs in a strong spatiotemporal context that is sensitive to environmental changes. In an open field environment, temperature fluctuates due to weather variations, accompanied by changes in factors such as moisture and light, making stable heat-stress conditions unfeasible. Therefore, we can only conduct the study under controlled conditions. Additionally, the tomato SAM is encased by multiple layers of leaf primordia with trichomes, preventing staining agents from directly entering the SAM cells. Microdissection under a stereoscope is required to remove these leaf primordia for staining and observation. Moreover, the instability and dynamic changes of cellular ROS also pose challenges for accurately measuring the endogenous ROS levels in plant cells. We can only maintain identical procedures for both the WT and mutant plants to obtain a relative quantification result to compare their differences.

RESOURCE AVAILABILITY

Lead contact

Further information and requests for resources and regents should be directed to, and will be fulfilled by, the lead contact, Cao Xu (caoxu@genetics.ac.cn).

Materials availability

The plasmids and the seeds of mutants and transgenic plants in this study can be made available on request.

Data and code availability

- All materials used in this study are available by contacting the corresponding authors.
- There is no original code in this paper.
- Additional data required for reanalysis of the findings presented in this paper can be obtained from the corresponding author upon request.

ACKNOWLEDGMENTS

We thank K. Jiang, J. Huang and P. Willems for kindly providing comments on the manuscript and L. Du and X. Fang for sharing the plasmids and yeast cells. This study was supported by grants from National Natural Science Foundation of China (31991183, 32225045, and 32270371) and the Youth Innovation Promotion Association of the Chinese Academy of Sciences (2022094).

AUTHOR CONTRIBUTIONS

C.X. designed and supervised the project. X.H., N.X., and Y.X. performed the experiments, analyzed the data, and prepared the figures. C.X. and X.H. wrote and revised the manuscript with input from N.X. All authors have read and approved the final manuscript.

DECLARATION OF INTERESTS

The authors declare no competing interests.

STAR★METHODS

Detailed methods are provided in the online version of this paper and include the following:

- KEY RESOURCES TABLE
- EXPERIMENTAL MODEL AND STUDY PARTICIPANT DETAILS
- METHOD DETAILS
  - Plant growth conditions
  - Heat treatment for tomato plants
  - Plasmid constructs and tomato transformation
  - Hydrogen peroxide and superoxide staining
  - Fluorescence microscopy of plants
  - Yeast fluorescence microscopy
  - Quantification of cells with puncta
  - Transcriptional activity assay
  - Image analysis and signal quantification
  - Tissue collection and RT-qPCR
  - Phase separation assay *in vitro*
- QUANTIFICATION AND STATISTICAL ANALYSIS

SUPPLEMENTAL INFORMATION

Supplemental information can be found online at https://doi.org/10.1016/j.devcel.2025.03.007.

Received: May 16, 2024
Revised: November 11, 2024
Accepted: March 10, 2025
Published: April 2, 2025

REFERENCES

1. Wang, X., Zhao, C., Müller, C., Wang, C., Ciais, P., Janssens, I., Peñuelas, J., Asseng, S., Li, T., Elliott, J., et al. (2020). Emergent constraint on crop yield response to warmer temperature from field experiments. Nat. Sustain. *3*, 908–916. https://doi.org/10.1038/s41893-020-0569-7.
2. Chaturvedi, P., Wiese, A.J., Ghatak, A., Záveská Drábková, L., Weckwerth, W., and Honys, D. (2021). Heat stress response mechanisms in pollen development. New Phytol. *231*, 571–585. https://doi.org/10.1111/nph.17380.
3. Pfeiffer, A., Wenzl, C., and Lohmann, J.U. (2017). Beyond flexibility: controlling stem cells in an ever changing environment. Curr. Opin. Plant Biol. *35*, 117–123. https://doi.org/10.1016/j.pbi.2016.11.014.

4. Moczek, A.P., Sultan, S., Foster, S., Ledón-Rettig, C., Dworkin, I., Nijhout, H.F., Abouheif, E., and Pfennig, D.W. (2011). The role of developmental plasticity in evolutionary innovation. Proc. Biol. Sci. *278*, 2705–2713. https://doi.org/10.1098/rspb.2011.0971.

5. de Jong, M., and Leyser, O. (2012). Developmental plasticity in plants. Cold Spring Harb. Symp. Quant. Biol. *77*, 63–73. https://doi.org/10.1101/sqb.2012.77.014720.

6. Meyerowitz, E.M. (1997). Genetic control of cell division patterns in developing plants. Cell *88*, 299–308. https://doi.org/10.1016/s0092-8674(00)81868-1.

7. Kazan, K., and Lyons, R. (2016). The link between flowering time and stress tolerance. J. Exp. Bot. *67*, 47–60. https://doi.org/10.1093/jxb/erv441.

8. Lippmann, R., Babben, S., Menger, A., Delker, C., and Quint, M. (2019). Development of wild and cultivated plants under global warming conditions. Curr. Biol. *29*, R1326–R1338. https://doi.org/10.1016/j.cub.2019.10.016.

9. Lohani, N., Singh, M.B., and Bhalla, P.L. (2020). High temperature susceptibility of sexual reproduction in crop plants. J. Exp. Bot. *71*, 555–568. https://doi.org/10.1093/jxb/erz426.

10. Sewelam, N., Kazan, K., and Schenk, P.M. (2016). Global plant stress signaling: reactive oxygen species at the cross-road. Front. Plant Sci. *7*, 187. https://doi.org/10.3389/fpls.2016.00187.

11. Considine, M.J., and Foyer, C.H. (2021). Stress effects on the reactive oxygen species-dependent regulation of plant growth and development. J. Exp. Bot. *72*, 5795–5806. https://doi.org/10.1093/jxb/erab265.

12. Dolzblasz, A., Smakowska, E., Gola, E.M., Sokołowska, K., Kicia, M., and Janska, H. (2016). The mitochondrial protease AtFTSH4 safeguards Arabidopsis shoot apical meristem function. Sci. Rep. *6*, 28315. https://doi.org/10.1038/srep28315.

13. Dolzblasz, A., Gola, E.M., Sokołowska, K., Smakowska-Luzan, E., Twardawska, A., and Janska, H. (2018). Impairment of meristem proliferation in plants lacking the mitochondrial protease AtFTSH4. Int. J. Mol. Sci. *19*, 853. https://doi.org/10.3390/ijms19030853.

14. Ding, H., He, J., Wu, Y., Wu, X., Ge, C., Wang, Y., Zhong, S., Peiter, E., Liang, J., and Xu, W. (2018). The tomato mitogen-activated protein kinase SlMPK1 is as a negative regulator of the high-temperature stress response. Plant Physiol. *177*, 633–651. https://doi.org/10.1104/pp.18.00067.

15. Yu, W., Wang, L., Zhao, R., Sheng, J., Zhang, S., Li, R., and Shen, L. (2019). Knockout of *SlMAPK3* enhances tolerance to heat stress involving ROS homeostasis in tomato plants. BMC Plant Biol. *19*, 354. https://doi.org/10.1186/s12870-019-1939-z.

16. Volkov, R.A., Panchuk, I.I., Mullineaux, P.M., and Schöffl, F. (2006). Heat stress-induced H_2O_2 is required for effective expression of heat shock genes in *Arabidopsis*. Plant Mol. Biol. *61*, 733–746. https://doi.org/10.1007/s11103-006-0045-4.

17. Zeng, J., Dong, Z., Wu, H., Tian, Z., and Zhao, Z. (2017). Redox regulation of plant stem cell fate. EMBO J. *36*, 2844–2855. https://doi.org/10.15252/embj.201695955.

18. Huang, X., Chen, S., Li, W., Tang, L., Zhang, Y., Yang, N., Zou, Y., Zhai, X., Xiao, N., Liu, W., et al. (2021). ROS regulated reversible protein phase separation synchronizes plant flowering. Nat. Chem. Biol. *17*, 549–557. https://doi.org/10.1038/s41589-021-00739-0.

19. Tsukagoshi, H., Busch, W., and Benfey, P.N. (2010). Transcriptional regulation of ROS controls transition from proliferation to differentiation in the root. Cell *143*, 606–616. https://doi.org/10.1016/j.cell.2010.10.020.

20. Banani, S.F., Lee, H.O., Hyman, A.A., and Rosen, M.K. (2017). Biomolecular condensates: organizers of cellular biochemistry. Nat. Rev. Mol. Cell Biol. *18*, 285–298. https://doi.org/10.1038/nrm.2017.7.

21. Franzmann, T.M., and Alberti, S. (2019). Protein phase separation as a stress survival strategy. Cold Spring Harb. Perspect. Biol. *11*, a034058. https://doi.org/10.1101/cshperspect.a034058.

22. Huang, X., Yang, Y., and Xu, C. (2025). Biomolecular condensation programs floral transition to orchestrate flowering time and inflorescence architecture. New Phytol. *245*, 88–94. https://doi.org/10.1111/nph.20204.

23. Kato, M., Yang, Y.S., Sutter, B.M., Wang, Y., McKnight, S.L., and Tu, B.P. (2019). Redox state controls phase separation of the yeast ataxin-2 protein via reversible oxidation of its methionine-rich low-complexity domain. Cell *177*, 711–721.e8. https://doi.org/10.1016/j.cell.2019.02.044.

24. Zavaliev, R., Mohan, R., Chen, T., and Dong, X. (2020). Formation of NPR1 condensates promotes cell Survival during the plant immune response. Cell *182*, 1093–1108.e18. https://doi.org/10.1016/j.cell.2020.07.016.

25. Erdős, G., Mészáros, B., Reichmann, D., and Dosztányi, Z. (2019). Large-scale analysis of redox-sensitive conditionally disordered protein regions reveals their widespread nature and key roles in high-level eukaryotic processes. Proteomics *19*, e1800070. https://doi.org/10.1002/pmic.201800070.

26. Dinar, M., and Rudich, J. (1985). Effect of heat-stress on assimilate partitioning in tomato. Ann. Bot. *56*, 239–248. https://doi.org/10.1093/oxfordjournals.aob.a087008.

27. Mishra, S.K., Tripp, J., Winkelhaus, S., Tschiersch, B., Theres, K., Nover, L., and Scharf, K.D. (2002). In the complex family of heat stress transcription factors, HSfA1 has a unique role as master regulator of thermotolerance in tomato. Genes Dev. *16*, 1555–1567. https://doi.org/10.1101/gad.228802.

28. Driedonks, N., Wolters-Arts, M., Huber, H., de Boer, G.J., Vriezen, W., Mariani, C., and Rieu, I. (2018). Exploring the natural variation for reproductive thermotolerance in wild tomato species. Euphytica *214*, 67. https://doi.org/10.1007/s10681-018-2150-2.

29. Park, S.J., Jiang, K., Schatz, M.C., and Lippman, Z.B. (2012). Rate of meristem maturation determines inflorescence architecture in tomato. Proc. Natl. Acad. Sci. USA *109*, 639–644. https://doi.org/10.1073/pnas.1114963109.

30. Lippman, Z.B., Cohen, O., Alvarez, J.P., Abu-Abied, M., Pekker, I., Paran, I., Eshed, Y., and Zamir, D. (2008). The making of a compound inflorescence in tomato and related nightshades. PLOS Biol. *6*, e288. https://doi.org/10.1371/journal.pbio.0060288.

31. Xu, C., Park, S.J., Van Eck, J., and Lippman, Z.B. (2016). Control of inflorescence architecture in tomato by BTB/POZ transcriptional regulators. Genes Dev. *30*, 2048–2061. https://doi.org/10.1101/gad.288415.116.

32. Wang, H., and Wang, H. (2015). The miR156/SPL module, a regulatory hub and versatile toolbox, gears up crops for enhanced agronomic traits. Mol. Plant *8*, 677–688. https://doi.org/10.1016/j.molp.2015.01.008.

33. Noctor, G., Reichheld, J.P., and Foyer, C.H. (2018). ROS-related redox regulation and signaling in plants. Semin. Cell Dev. Biol. *80*, 3–12. https://doi.org/10.1016/j.semcdb.2017.07.013.

34. Mittler, R., Zandalinas, S.I., Fichman, Y., and Van Breusegem, F. (2022). Reactive oxygen species signalling in plant stress responses. Nat. Rev. Mol. Cell Biol. *23*, 663–679. https://doi.org/10.1038/s41580-022-00499-2.

35. Frisch, J., Angenendt, A., Hoth, M., Prates Roma, L.P., and Lis, A. (2019). STIM-orai channels and reactive oxygen species in the tumor microenvironment. Cancers (Basel) *11*, 457. https://doi.org/10.3390/cancers11040457.

36. MacAlister, C.A., Park, S.J., Jiang, K., Marcel, F., Bendahmane, A., Izkovich, Y., Eshed, Y., and Lippman, Z.B. (2012). Synchronization of the flowering transition by the tomato *TERMINATING FLOWER* gene. Nat. Genet. *44*, 1393–1398. https://doi.org/10.1038/ng.2465.

37. Wang, B., Zhang, H., Huai, J., Peng, F., Wu, J., Lin, R., and Fang, X. (2022). Condensation of SEUSS promotes hyperosmotic stress tolerance in *Arabidopsis*. Nat. Chem. Biol. *18*, 1361–1369. https://doi.org/10.1038/s41589-022-01196-z.

38. Riback, J.A., Katanski, C.D., Kear-Scott, J.L., Pilipenko, E.V., Rojek, A.E., Sosnick, T.R., and Drummond, D.A. (2017). Stress-triggered phase separation is an adaptive, evolutionarily tuned response. Cell *168*, 1028–1040.e19. https://doi.org/10.1016/j.cell.2017.02.027.

39. Delarue, M., Brittingham, G.P., Pfeffer, S., Surovtsev, I.V., Pinglay, S., Kennedy, K.J., Schaffer, M., Gutierrez, J.I., Sang, D., Poterewicz, G.,

et al. (2018). mTORC1 controls phase separation and the biophysical properties of the cytoplasm by tuning crowding. Cell *174*, 338–349.e20. https://doi.org/10.1016/j.cell.2018.05.042.

40. Jung, J.H., Barbosa, A.D., Hutin, S., Kumita, J.R., Gao, M.J., Derwort, D., Silva, C.S., Lai, X., Pierre, E., Geng, F., et al. (2020). A prion-like domain in ELF3 functions as a thermosensor in *Arabidopsis*. Nature *585*, 256–260. https://doi.org/10.1038/s41586-020-2644-7.
41. Li, C., Zong, Y., Wang, Y., Jin, S., Zhang, D., Song, Q., Zhang, R., and Gao, C. (2018). Expanded base editing in rice and wheat using a Cas9-adenosine deaminase fusion. Genome Biol. *19*, 59. https://doi.org/10.1186/s13059-018-1443-z.
42. Richter, M.F., Zhao, K.T., Eton, E., Lapinaite, A., Newby, G.A., Thuronyi, B.W., Wilson, C., Koblan, L.W., Zeng, J., Bauer, D.E., et al. (2020). Phage-assisted evolution of an adenine base editor with improved Cas domain compatibility and activity. Nat. Biotechnol. *38*, 883–891. https://doi.org/10.1038/s41587-020-0453-z.
43. Čermák, T., Curtin, S.J., Gil-Humanes, J., Čegan, R., Kono, T.J.Y., Konečná, E., Belanto, J.J., Starker, C.G., Mathre, J.W., Greenstein, R.L., et al. (2017). A multipurpose toolkit to enable advanced genome engineering in plants. Plant Cell *29*, 1196–1217. https://doi.org/10.1105/tpc.16.00922.
44. Rosenfeld, J.A., Coe, B.P., Eichler, E.E., Cuckle, H., and Shaffer, L.G. (2013). Estimates of penetrance for recurrent pathogenic copy-number variations. Genet. Med. *15*, 478–481. https://doi.org/10.1038/gim.2012.164.
45. Huang, X., Qian, Q., Liu, Z., Sun, H., He, S., Luo, D., Xia, G., Chu, C., Li, J., and Fu, X. (2009). Natural variation at the locus enhances grain yield in rice. Nat. Genet. *41*, 494–497. https://doi.org/10.1038/ng.352.
46. Wu, Q., Regan, M., Furukawa, H., and Jackson, D. (2018). Role of heterotrimeric Gα proteins in maize development and enhancement of agronomic traits. PLOS Genet. *14*, e1007374. https://doi.org/10.1371/journal.pgen.1007374.
47. Park, S.J., Eshed, Y., and Lippman, Z.B. (2014). Meristem maturation and inflorescence architecture - lessons from the Solanaceae. Curr. Opin. Plant Biol. *17*, 70–77. https://doi.org/10.1016/j.pbi.2013.11.006.
48. Huang, X., Xiao, N., Zou, Y., Xie, Y., Tang, L., Zhang, Y., Yu, Y., Li, Y., and Xu, C. (2022). Heterotypic transcriptional condensates formed by prion-like paralogous proteins canalize flowering transition in tomato. Genome Biol. *23*, 78. https://doi.org/10.1186/s13059-022-02646-6.
49. Fouracre, J.P., and Poethig, R.S. (2020). Lonely at the top? Regulation of shoot apical meristem activity by intrinsic and extrinsic factors. Curr. Opin. Plant Biol. *58*, 17–24. https://doi.org/10.1016/j.pbi.2020.08.008.
50. Andrés, F., and Coupland, G. (2012). The genetic basis of flowering responses to seasonal cues. Nat. Rev. Genet. *13*, 627–639. https://doi.org/10.1038/nrg3291.
51. Ichihashi, Y., Hakoyama, T., Iwase, A., Shirasu, K., Sugimoto, K., and Hayashi, M. (2020). Common mechanisms of developmental reprogramming in plants-lessons from regeneration, symbiosis, and parasitism. Front. Plant Sci. *11*, 1084. https://doi.org/10.3389/fpls.2020.01084.
52. Sugimoto, K., Xu, L., Paszkowski, U., and Hayashi, M. (2018). Multifaceted cellular reprogramming at the crossroads between plant development and biotic interactions. Plant Cell Physiol. *59*, 651–655. https://doi.org/10.1093/pcp/pcy066.
53. Alberti, S., Gladfelter, A., and Mittag, T. (2019). Considerations and challenges in studying liquid-liquid phase separation and biomolecular condensates. Cell *176*, 419–434. https://doi.org/10.1016/j.cell.2018.12.035.
54. Nover, L., Scharf, K.D., and Neumann, D. (1983). Formation of cytoplasmic heat-shock granules in tomato cell-cultures and leaves. Mol. Cell. Biol. *3*, 1648–1655. https://doi.org/10.1128/mcb.3.9.1648-1655.1983.
55. Zhu, S., Gu, J., Yao, J., Li, Y., Zhang, Z., Xia, W., Wang, Z., Gui, X., Li, L., Li, D., et al. (2022). Liquid-liquid phase separation of RBGD2/4 is required for heat stress resistance in *Arabidopsis*. Dev. Cell *57*, 583–597.e6. https://doi.org/10.1016/j.devcel.2022.02.005.
56. Chen, D., Lyu, M., Kou, X., Li, J., Yang, Z., Gao, L., Li, Y., Fan, L.M., Shi, H., and Zhong, S. (2022). Integration of light and temperature sensing by liquid-liquid phase separation of phytochrome B. Mol. Cell *82*, 3015–3029.e6. https://doi.org/10.1016/j.molcel.2022.05.026.
57. Vogelsang, L., and Dietz, K.J. (2022). Plant thiol peroxidases as redox sensors and signal transducers in abiotic stress acclimation. Free Radic. Biol. Med. *193*, 764–778. https://doi.org/10.1016/j.freeradbiomed.2022.11.019.

Please cite this article in press as: Huang et al., ROS burst prolongs transcriptional condensation to slow shoot apical meristem maturation and achieve heat-stress resilience in tomato, Developmental Cell (2025), https://doi.org/10.1016/j.devcel.2025.03.007

STAR★METHODS

KEY RESOURCES TABLE

REAGENT or RESOURCE	SOURCE	IDENTIFIER
Bacterial and virus strains		
Escherichia coli: *DH5α*	This paper	N/A
Escherichia coli: *Rosetta* (*DE3*)	WEIDI	Cat#: EC1010
Agrobacterium tumefaciens: *AGL1*	WEIDI	Cat#: AE1020
Fission yeast strain: *LD328*	Wang et al.[36]	N/A
Chemicals, peptides, and recombinant proteins		
DAB	Sigma-Aldrich	Cat#: D8001
NBT	Sigma-Aldrich	Cat#: N5514
HPF	Cayman Chemical	Cat#: 10159
Low Melting Point Agarose	VWR Chemicals	Cat#: 0815
Paraformaldehyde	Sigma-Aldrich	Cat#: 158127
4-Methylumbelliferyl -β-D-glucuronide hydrate (MUG)	Sigma-Aldrich	Cat#: M9130
Critical commercial assays		
CloneExpress II One Step Cloning Kit	Vazyme	Cat#: C11202
Arcturus PicoPure RNA Isolation Kit	Thermo Scientific	Cat#: 12204-01
Luciferase 1000 Assay System	Promega	Cat#: E4550
Experimental models: Organisms/strains		
Tomato cultivar: AC	This paper	N/A
Tomato cultivar: M82	This paper	N/A
M82: *tmf-2*	MacAlister et al.[35]	N/A
M82: *tmf-1*	MacAlister et al.[35]	N/A
M82: *35S:GFP-TMF/tmf*	This paper	N/A
M82: *35S:GFP-TMF^{C112S}/tmf*	Huang et al.[18]	N/A
M82: *35S:GFP-TMF*	Huang et al.[18]	N/A
AC: *Slrboh1 Slrboh2*	Huang et al.[18]	N/A
AC: *CR-SlPRX1*	This paper	N/A
M82: *CR-SlPRX2*	This paper	N/A
M82: *CR-TMF^{C124R}*	This paper	N/A
M82: *pTMF:SlRBOH1-GFP*	This paper	N/A
Nicotiana benthamiana: tobacco	This paper	N/A
Oligonucleotides		
See Table S1	N/A	N/A
Software and algorithms		
Fiji	NIH	https://imagej.net/software/fiji/downloads
Prism	GraphPad	https://www.graphpad.com/features
Adobe illustrator	Adobe	https://www.adobe.com/

EXPERIMENTAL MODEL AND STUDY PARTICIPANT DETAILS

The tomato (*Solanum lycopersicum*) cultivar Ailsa Craig (AC) and M82 were used in this study. The *Slrboh1 Slrboh2* mutant generated in AC was used in the previous study.[18] *tmf-1* and *tmf-2* mutants were shared by Z. B. Lippman (Cold Spring Harbor Laboratory). *CR-SlPRX1* mutant was generated in AC, and *CR-SlPRX2*, *CR-TMF^{C124R}* mutants were generated in M82, and *35S:GFP-TMF/tmf* transgenic plants generated in *tmf* mutant background by Agrobacterium-mediated tissue culture, respectively. Under normal condition, plants were grown in growth room with a 16-hour light/8-hour dark photoperiod at 26°C and 45-60% relative humidity, under LED lighting (Philips Lighting IBRS) with an intensity of 80-100 μmol m^2 s^{-1}.

Please cite this article in press as: Huang et al., ROS burst prolongs transcriptional condensation to slow shoot apical meristem maturation and achieve heat-stress resilience in tomato, Developmental Cell (2025), https://doi.org/10.1016/j.devcel.2025.03.007

METHOD DETAILS

Plant growth conditions

For plant cultivation, seeds were germinated on filter paper for three days in dark at room temperature, and then were sown into soil in growth room. Under normal condition, plants were grown in growth room with 16 hours of light and 8 hours of dark at 26°C, 45-60% relative humidity under LED (Philips Lighting IBRS) light with 80-100 μmol m^2 s^{-1} light intensity.

Heat treatment for tomato plants

Heat treatment for tomato plants was conducted in a plant growth chamber (CONVIRON CMP6010) with 16 hours of light at 35°C and 8 hours of dark at 28°C, 50% relative humidity and 80-100 μmol m^2 s^{-1} light intensity. For heat treatment in Figure 1, the plants at EVM stage grown under normal condition were selected and transferred to the plant growth chamber for continuous heat treatment, where they were allowed to grow until MVM, LVM, TM, and FM stages. For heat treatment in Figure 2, the plants at EVM, MVM, LVM, TM, and FM stages grown under normal condition were simultaneously selected and transferred to the plant growth chamber for 14-day heat treatment. For the heat treatment of *Slrboh1 Slrboh2*, *tmf-1*, *tmf-2*, *CR-TMF*^{C124R} mutants and corresponding wild-types, the plants at EVM stage were selected and transferred to the plant growth chamber for heat treatment. The duration time of heat treatment across all experiments is determined by the specific developmental stage of WT or mutant plants as described in main text and figure legends. Following heat treatment, the plants were transplanted to a growth room under normal condition for recovery growth and subsequent phenotypic analysis, with plants continuously grown under normal condition serving as controls.

Plasmid constructs and tomato transformation

To generate the *pDIRECT-22C-ABE8e* vector, the Asp (D) at position 10 of Cas9 in *pDIRECT-22C* was mutated to Ala (A) to generate nCas9, then the coding sequence of tRNA adenosine deaminase TadA-8e with a 34 aa linker sequence synthesized by the Beijing Genomics Institute (BGI) was amplified and constructed at the N-terminus of nCas9.[42] The target-sgRNA expression cassettes were then cloned into *pDIRECT-22C-ABE8e* for base editing by using the same construct protocol as gene editing of *pDIRECT-22C* vector system.[43]

To generate *35S:GFP-TMF* transgenic plants, the coding sequence of *TMF* was amplified using the primer listed in Table S1 and ligated into the *PRI101-GFP* vector by In-Fusion cloning. To produce *pTMF:SlRBOH1-YFP* transgenic plants, the 3-kb fragment upstream of the transcription start site of *TMF* was amplified and cloned into *pGWB401*, with the *SlRBOH1* coding sequence fused with *YFP* at C terminal, using In-Fusion cloning (TransGen Biotech). The completed constructs were transformed into M82 plants by Agrobacterium-mediated transformation.

Hydrogen peroxide and superoxide staining

To visualize ROS accumulation, fluorescence probe HPF (Alexis Biochemical), chemical dye DAB (Sigma-Aldrich) and NBT (Sigma) were used. For HPF staining, tomato seedlings at transition meristem (TM) stage with or without heat stress treatment were dissected to remove extra leaves and embedded in 6% agarose (VWR Chemicals). The embedded materials were sectioned to a thickness of 50 μm using microtome (Leica VT1200S) and incubated for 5 min in phosphate buffered saline (PBS) containing 5 μM HPF in the dark at room temperature. For DAB staining, young true leaves of tomato seedlings with or without heat stress treatment were excised and incubated in DAB staining buffer (1 mg/ml DAB and 10 mM Na_2HPO_4 at pH 6.5) for 26 h in the dark. After staining, leaves were fixed and destained in bleaching solution of 3:1:1 ethanol:lactic acid:glycerol. For NBT staining, young true leaves of tomato seedlings with or without heat stress treatment were incubated in the NBT staining buffer (1 mg/ml NBT and 50 mM KH_2PO_4, pH 7.6) for 26 h in the dark, then fixed and destained in the bleaching solution of 3:1:1 ethanol:lactic acid:glycerol. The area and color exhibited on the leaves stained by DAB and NBT indicate the level of ROS.

Fluorescence microscopy of plants

The tomato *35S:GFP-TMF/tmf* and *35S:GFP-TMF*^{C112S}*/tmf* transgenic plants were grown in a growth room at 26°C, and then half of plants were transferred to plant growth chamber at 35°C for 3-days heat stress treatment. Tomato seedlings at transition meristem (TM) stage with or without heat stress treatment were dissected to remove extra leaves and fixed with 4% Paraformaldehyde (PFA, Sigma), and then embedded in 6% agarose (VWR Chemicals). The embedded materials were sectioned to a thickness of 50 μm using microtome (Leica VT1200S). Sectioned meristems were imaged using a Zeiss LSM980 confocal microscope with 20×, 40× objectives. The tomato *35S:GFP-TMF* transgenic plants were grown in a growth room at 26°C. Detached leaves were imaged before and after incubation at 37°C for 1 h using a Zeiss LSM980 confocal microscope with 20×, 40× objectives. For transient expression of GFP-TMF and GFP-TMF^{C112S} in tobacco leaves, *N. benthamiana* (tobacco) leaves were infiltrated with Agrobacterium *AGL1* containing *35S:GFP-TMF* or *35S:GFP-TMF*^{C112S} plasmid, respectively. After 48 h, detached tobacco leaves were imaged before and after incubation at 37°C for 30 min using a Zeiss LSM980 confocal microscope with 20×, 40× objectives. GFP fluorescence was excited at 488 nm and detected at 500–540 nm.

Yeast fluorescence microscopy

The coding sequence of TMF fused GFP was amplified and cloned into *pDUAL-Pnmt1-yeGFP* vector by In-fusion cloning. The GFP-TMF protein was expressed in the fission yeast strain *LD328* as the following protocol. Yeast cells were cultured in YES medium until OD_{600}

Please cite this article in press as: Huang et al., ROS burst prolongs transcriptional condensation to slow shoot apical meristem maturation and achieve heat-stress resilience in tomato, Developmental Cell (2025), https://doi.org/10.1016/j.devcel.2025.03.007

reached 0.4–0.8, then collected and washed with sterilized water for three times and resuspended in buffer I (240 μL included 50% PEG3350, 36 μL of LiAc (1.0 M) and 10 μL of boiled single-stranded carrier DNA (10 mg ml^{-1})). The plasmids were digested with NotI restriction enzyme, and the products were purified. The resuspended cells were then added to 34 μL of the linearized plasmid (up to 1 μg), mixed vigorously, and incubated at 42°C for 40 min. The cells were centrifuged, resuspended with 100 μL water and plated on EMM + HT (EMM medium supplemented with 45 mg L^{-1} histidine and 15 μM thiamine) solid medium. After incubation at 30°C for 3-5 days, 5-10 individual colonies were picked and refreshed by drawing lines on the YES solid medium. After incubation at 30°C for 1-2 d, yeast cells were transferred to EMM + H (EMM medium supplemented with 45 mg L^{-1} histidine) plates and cultured overnight at 30°C. The cells were imaged before and after incubation at 37°C for 30 min using a Zeiss LSM980 confocal microscope equipped with 63× objectives.

Quantification of cells with puncta

To assess the puncta state in cells, we set the GFP signals in the nucleus with heterogeneity characteristic as the presence of puncta and vice versa as no puncta.[18,47] We quantified the percentage of the cells with puncta to reflect the phase separation capacity of TMF and TMF^{C112S}.

Transcriptional activity assay

The GUS–LUC dual reporter system was used for transcriptional activity analysis in this study. The TMF protein fused GFP served as an effector, while GFP alone served as a negative control. The *GUS* gene driven by the 2-kb upstream promoter of *AN* (*pAN:GUS*) was used as a reporter, and the *LUC* gene driven by the *CaMV 35S* promoter (*35S:LUC*) served as an internal control. The Agrobacterium was cultured overnight in liquid LB medium at 28°C, and then diluted to an OD_{600} of 0.8. The Agrobacterium strains expressing different proteins were mixed together in a specific ratio, with the following composition (1.2 mL): 300 μL P19 + 4 μL internal control + 300 μL reporter + 600 μL effector. The combinations were co-infiltrated into *Nicotiana benthamiana* leaves as indicated, respectively. After 48 h, half of the infiltrated leaves were treated with 35°C for 12 h before harvesting, while the untreated leaves were harvested as a control. The substrates 4-methylumbelliferyl glucuronide (Sigma) and luciferin (Promega) were used to measure the activity of GUS and luciferase (LUC), respectively. The ratio of GUS/LUC was used to reflect the transcriptional activity.

Image analysis and signal quantification

Meristem samples were imaged with a fluorescence microscope (Leica DM2500) and leaves were photographed using a digital single-lens reflex camera. The relative intensity of ROS staining in entire leaf or meristem was quantified using ImageJ (Fiji Win64). Images were converted to grayscale, and the intensity was measured according to the software's user guide.

Tissue collection and RT-qPCR

Seedlings at the EVM stage grown at 26°C were selected and transferred to plant chamber with 16 h light at 35°C and 8 h dark at 28°C and 50% relative humidity for heat treatment. The primary meristems at TM stage from tomato seedlings grown under normal condition and heat treatment were collected using hand microdissection. Total RNA was extracted using the Arcturus PicoPure RNA Isolation Kit (Thermo, 00860267), cDNA was generated by reverse transcription PCR with SuperScript IV Reverse Transcriptase (Invitrogen, 18090010), and RT-qPCR was performed with TB green Prexim Ex Taq (Takara, RR820A). The primers are listed in Table S1.

Phase separation assay *in vitro*

The coding sequences of GFP-TMF and GFP-TMF^{C124R} were cloned separately into the *pQE-80L* vector, and the resulting constructs were transformed into *E. coli* Rosetta (DE3) competent cells. Positive clones were cultured in LB medium and protein expression was induced with 0.5 mM isopropyl β-D-1-thiogalactopyranoside (IPTG) for 16 h at 16 °C. After harvesting the cells, purification was carried out using Ni-NTA affinity beads (GE Healthcare). The eluted proteins were subsequently subjected to buffer exchange and concentration using Vivaspin Turbo ultrafiltration tubes. Purified proteins were stored in a buffer containing 50 mM Tris-HCl and 200 mM NaCl, pH 7.4. For phase separation assays, proteins were diluted into a buffer containing 50 mM Tris-HCl (pH 7.4) and 25 mM NaCl to the final concentrations specified in the figure legends. The diluted protein solutions were incubated for 15 minutes at room temperature in a 384-well plate. Droplet was imaged with a Leica SP5 confocal microscope equipped with a 20× objective. GFP fluorescence was excited at 488 nm and detected at 500–540 nm.

QUANTIFICATION AND STATISTICAL ANALYSIS

Statistical details for each analysis, including the statistical tests used, exact sample size (N), what N represents, definition of center, and dispersion measures, are provided in the respective figures and figure legends. Comparisons between two groups were performed using unpaired two-tailed Student's t-tests, and statistical analyses were conducted using GraphPad Prism 8.0.2. Results are presented as mean ± standard deviation. Significance levels are indicated in the figures as follows: $^{*}P < 0.05$, $^{**}P < 0.01$, and $^{***}P < 0.001$. Data were assessed for normal distribution, and no significant differences in variance were observed between groups in individual comparisons. The source data used for quantification and statistical analysis are listed in Table S2.